



## Fabrication of FTO(P)/ZNS(P)/SI(N) Heterojunction and Study of Its Structural, Optical and Electrical Properties

Ahmad Aljader \* **emil:** [ahmad.eref.aljader.84@gmail.com](mailto:ahmad.eref.aljader.84@gmail.com)

Mohamed Anwar Batal\*\*, Mohamed Bashir Karaman\*\*

\*PHD student, Dept. of physics, Faculty of Science, University. Of Aleppo.

\*\* Prof. Dept. of physics, Faculty of Science, University. Of Aleppo.

### Abstract

To make a heterojunction of FTO(p)/ZnS(p)/Si(n), first: FTO(p) was prepared using the thermal spraying method in order to deposit the FTO(P) layer on a glass slide, second: A semiconductor of ZnS(p) was prepared by the electrochemical deposition method in order to deposit it on the FTO(p) layer, and then the sample was treated to FTO(p)/ZnS(p) at a temperature of (150) C<sup>0</sup> in a vacuum tube furnace, then it was attached to a Si(n) slide. Atomic force microscopy (AFM) showed surface images of the FTO(p)/ZnS(p) sample with dimensions of (48.5μm x 48.5μm), where the average atomic clusters appeared (89.3) nm with a semi-homogeneous granular structure, and the average surface heights of the granular cluster on the junction surface were (90.7) nm, indicating the formation of a homogeneous structure. X-ray diffraction measurements showed that the FTO(p)/ZnS(p) composite crystallized according to the hexagonal structure by electrochemical deposition method. The optical absorption spectrum of the FTO(p) substrate showed a sharp absorption peak corresponding to the wavelength of 306nm which corresponds to the energy gap (4.05) ev, and the optical absorption spectrum of the semiconductor ZnS(p) showed several optical absorption peaks corresponding to the wavelengths, indicating the presence of multiple impurity levels within the energy gap formed because of doping. The optical absorption spectrum of the FTO(P)/ZnS(p) sample was measured, where the optical absorption spectrum shows the presence of several optical absorption peaks within the visible and infrared range corresponding to several wavelengths, because of the overlap of energy levels during the deposition process in addition to the repositioning of the impurity levels within the forbidden band width of the semiconductor ZnS(p). The type of semiconductor FTO(p)/ZnS(p) was confirmed experimentally by studying the changes in the reciprocal square of the electrical capacitance in function of the applied potential. The I-V characteristic of the FTO(p)/ZnS(p)/Si(n) heterojunction showed a decrease in the threshold potential value when the junction surface is illuminated, with a constant saturation current in the reverse bias



condition, which is identical to the diode condition. The ideality factor of the junction was calculated, and its value was very high ( $n=163$ ), indicating the dominance of tunneling electronic transitions.

**Keywords:** FTO(p), ZnS(p), AFM, UV, PL, XRD, I-V.

## **1- Introduction:**

A heterojunction is generally defined as an adhesion between two different types of materials and is usually defined in semiconductor research as a junction between two different materials of single-crystal or polycrystalline semiconductors. Such junctions can be classified as abrupt junctions or graded junctions according to the distances over which the charge carriers move from one end to the other. For example, in the case of abrupt junctions, the transfer occurs

within small atomic distances ( $\approx 1\text{nm}$ ), while in the case of graded junctions, the charge carriers move several wavelengths accompanying the diffusion of the charge carriers. Another classification for the junctions formed between semiconductors includes naming the heterojunction according to the type of conductivity on both sides of the contact region. If the two semiconductors involved have similar types of conductivity, the junction is called an isotype heterojunction; otherwise, it is called an anisotype heterojunction (Heterojunction Bipolar Transistor HBT) [1-2-3]. However, the study of heterojunction bonding was not taken up until Cromer proposed it [4]. Anisotype heterojunctions may exhibit extremely high injection efficiencies compared to homojunctions. The first symmetric anisotype heterojunction was fabricated by Anderson in 1960 [5]. He also provided a more detailed model for the energy level alignment near the contact region between semiconductors [6]. These types of heterojunctions include n-p and p-n heterojunctions, and there are a few devices like n-p or p-n junctions. Unlike the model proposed by Shockley for homojunctions, none of the numerous models proposed by various researchers can explain nearly all the physical phenomena of such heterojunctions [7], because in the case of heterojunctions, the contact properties vary significantly from one material to another and depend greatly on the method of formation and bonding. The existing models for anisotype differences can be considered extensions of the traditional homojunction model.



## 2- Importance of the Research and Its Objectives:

Heterojunctions are of great importance due to their wide applications in the field of electronics and optoelectronics. The (p-n) heterojunctions have broad applications, especially in photodetectors and light emission, and they are easy to fabricate using different methods.

## 3- Experimental study:

### 3-1-Devices and tools used:

- Sensitive electronic balance. SARTORIUS.
- Magnetic mixer.
- X-ray unit. (PHYWE Systeme GmbH & Co. KG).
- PL. (Scinco)
- DC. power supply.
- AFM. (Nanosurf Naio AFM).

### 3-2-FTO(p)/ZnS(p)/Si(n) heterojunction preparation stages:

A heterojunction of FTO(p)/ZnS(p)/Si(n) was prepared using the thermal spray method to deposit the FTO(P) layer on a glass slide, and the electrochemical deposition method to deposit the ZnS(p) layer on the FTO(p) layer.

The following is the method of preparing the junction as follows:

#### First: Preparation of a transparent semiconductor glass slide of FTO(p):

A transparent semiconductor glass slide of FTO(p) was prepared by dissolving (6.5 gr) of tin chloride in (50 ml) of ethanol using a magnetic stirring mixer. When the dissolution was complete, (0.35 gr) of fluoric acid was added to the mixture, resulting in a transparent FTO(n) solution, and by mixing the previous solution with 5% of iron chloride solution to produce a green solution of FTO(p). The glass slides were cleaned with potassium chromate solution, then washed with distilled water, then immersed in fluoric acid for (5 min) to scratch the surface of the slides, then washed with ethanol, and then dried in a thermal drying oven. After complete drying, the glass slides were heated on the surface of an electric heater. When the temperature of the glass slide reached (C0400), the surface of the slides was sprayed (5 ml) of the solution with a very small diameter (1 mm) spray jet at a rate of covering every (7 min) and for eight times. The electrical resistance of the slides was measured and found to range between (18-13)  $\Omega$  [8].



## Second: Preparation of a self-conducting semiconductor from ZnS with a conductivity of the type (P):

Dissolve 0.02 M of zinc sulfate ((ZnSO<sub>4</sub>,7H<sub>2</sub>O)) in 50 ml of distilled water with continuous stirring using a magnetic mixer for 10 min, then dissolve 0.2 M of sodium thiosulfate (Na<sub>2</sub>S<sub>2</sub>O<sub>3</sub>,5H<sub>2</sub>O) in 50ml of distilled water with continuous stirring using a magnetic mixer for 10min. The two solutions are placed in one beaker with continuous stirring for 10min. While stirring, 4 drops of triethanolamine (TEA) are added, equivalent to (3%) of the mass of (ZnSO<sub>4</sub>,7H<sub>2</sub>O) and (Na<sub>2</sub>S<sub>2</sub>O<sub>3</sub>,5H<sub>2</sub>O), then several drops of sulfuric acid H<sub>2</sub>SO<sub>4</sub> are added to make the PH value = 3 for the solution, as triethanolamine (TEA) is used to control the acidity in the reaction (adjust the pH), and it also reduces the surface tension of the solution and maintains the stability and effectiveness of the solution [9]. The prepared FTO(P) chip was immersed in the solution and connected to the negative pole of a voltage supply (cathode), then a graphite rod was immersed and connected to the positive pole of the voltage supply, so that the applied DC voltage difference was 2V and the distance between the two poles was 2cm. After 45min, we observed the deposition of zinc sulfide on the FTO(P) chip. Then the FTO(P)/ZnS(p) sample was washed with distilled water and treated at (100C0) for 2h in a tubular furnace evacuated from air by a mechanical pump that provides low pressure up to (0.001 mbar).

## Third: Heterogeneous junction FTO(p)/ZnS(p)/Si(n):

A silicon chip {with conductivity (n), crystal orientation (111), specific resistance (0.002-100) and thickness (360-400) mm} doped with phosphorus was attached to the FTO(P)/ZnS(p) chip as shown in Figure (1).

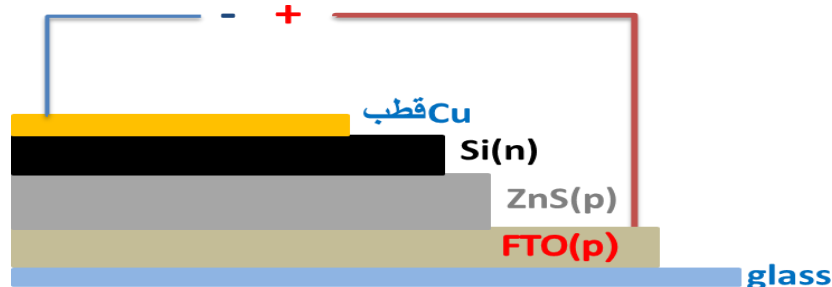


Figure (1): Heterojunction structure FTO(p)/ZnS(p)/Si(n)



### 3-3 Experimental measurements, results and discussion: 3-3-1

#### Study of structural properties:

##### 3-3-1-1 Atomic force microscope (AFM) images:

Using the atomic force microscope, surface images of the FTO(p)/ZnS(p) sample were taken with dimensions of (48.5 $\mu$ m x 48.5 $\mu$ m). As shown in Figure (2), the average atomic clusters appear (89.3) nm with the appearance of a semi-homogeneous granular structure.

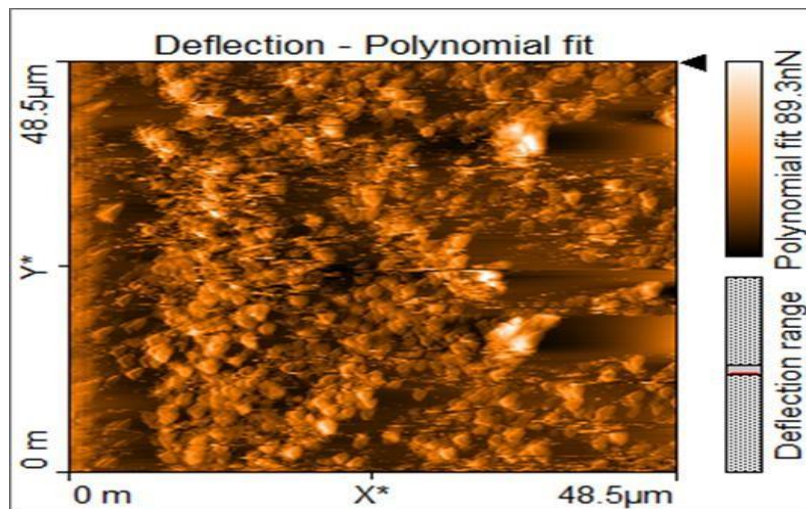


**Figure (2) AFM images of the surface structure of the FTO(p)/ZnS(p) junction.**

The average surface heights of the grain aggregation on the junction surface were (90.7) nm, indicating the formation of a homogeneous structure.

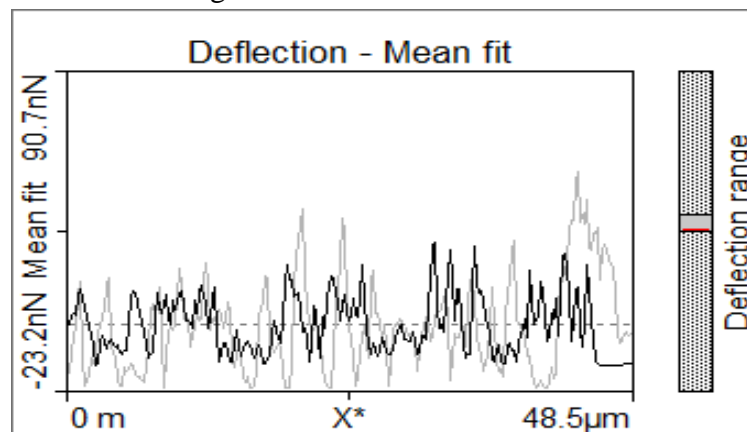


**Figure (3) Average surface heights of the grains formed on the surface of the FTO(p)/ZnS(p) junction.**



### 3-3-1-2- X-ray diffraction spectrum of FTO(p)/ZnS(p):

Using an X-ray spectrometer, the X-ray diffraction spectrum of the FTO(p)/ZnS(p) heterojunction was taken within the angular range (10-80) deg. Figure (4) shows the appearance of peaks of several crystalline diffraction levels.

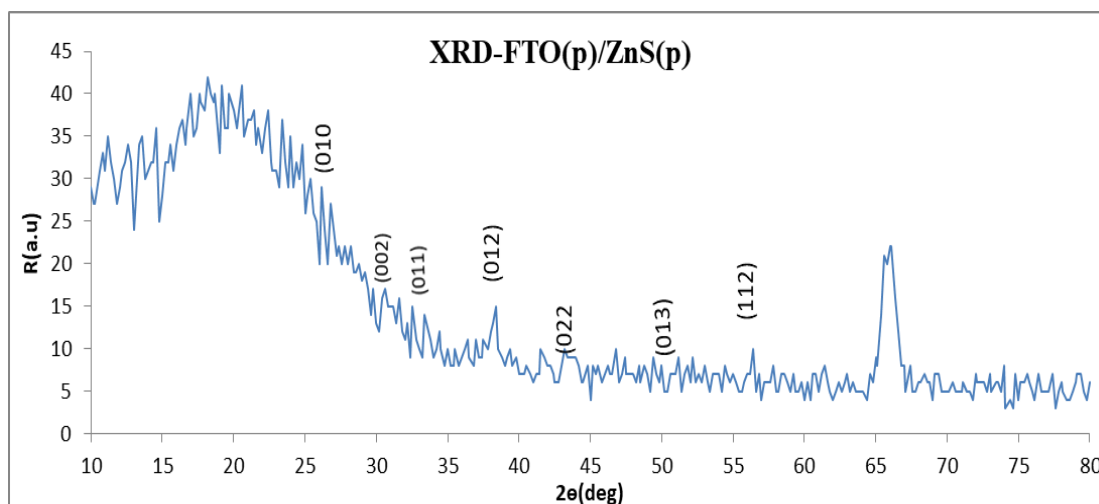


Figure (4) X-ray diffraction spectrum of FTO/ZnS(p) junction.

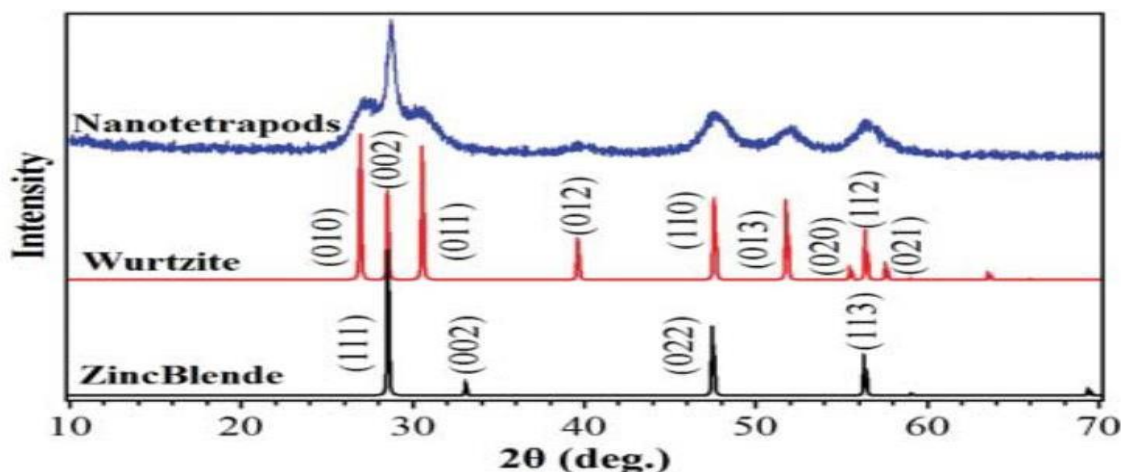


Figure (5) Reference diffraction levels of zinc sulfide compound crystallized according to the hexagonal and cubic structure.

By comparing the experimental diffraction peaks with Figure (5), we find that zinc sulfide compound crystallizes according to the hexagonal structure [10]. The crystallization size of the



zinc sulfide crystals formed can also be calculated based on the Debye-Scherrer equation [11]:

$$D = \frac{k \lambda}{\beta_{hkl} \cos\theta_{hkl}}$$

where  $k$  is a constant of 0.9,  $\lambda$  is the wavelength of the X-rays, and  $\beta$  is the intensity width at the midpoint of the diffraction peak corresponding to the crystal plane (hkl). Taking the most oriented plane (012):

$$D = \frac{0.9 \times 1.5418}{0.003 \times \cos(19.1)} = 489.4A = 48.9 \text{ nm}$$

The average stress in the formed ZnS crystals can also be calculated based on the following relationship [12]:

$$\varepsilon = \left[ \frac{\lambda_{cuk}}{a} - \beta_{hkl} \right] \times \frac{1}{D(\cos\theta) \tan\theta}$$

$$\varepsilon = \left[ \frac{1.5418}{489.4 \times \cos(19.1)} - 0.003 \right] \times \frac{1}{\tan(19.1)} = 0.34 \text{ lin}^2. \text{ m}^{-4}$$

The density of dislocations in the formed crystal structure can also be calculated based on the following [11]:

$$\delta = \frac{1}{D^2}$$

$$\delta = \frac{1}{(48.9 \text{ nm})^2} = 41.8 \times 10^{-3} \text{ lin. nm}$$



(48.9)<sup>2</sup>

Table (3-3) summarizes the results of the structural study that was calculated.

hkl	$\theta$ (deg)	D(nm)	$\ln^2 .m^{-4}$ ) $\theta$ )	$(\ln.nm)$ $\theta$
012	19.1	48.9	0.34	0.0418

### 3-3-2 Optical properties:

The optical properties of the prepared junction were studied by studying the absorption and optical fluorescence spectra of each layer of the junction and then measuring the optical absorption spectrum of the junction after the deposition process.

#### 3-3-2-1 Optical absorption spectrum of the FTO(p) junction:

The optical absorption spectrum of the FTO(p) substrate was taken within the wavelength (200-800) nm as shown in Figure (6). The absorption spectrum shows the presence of a sharp absorption peak corresponding to the wavelength 306 nm corresponding to the energy (4.05) ev.

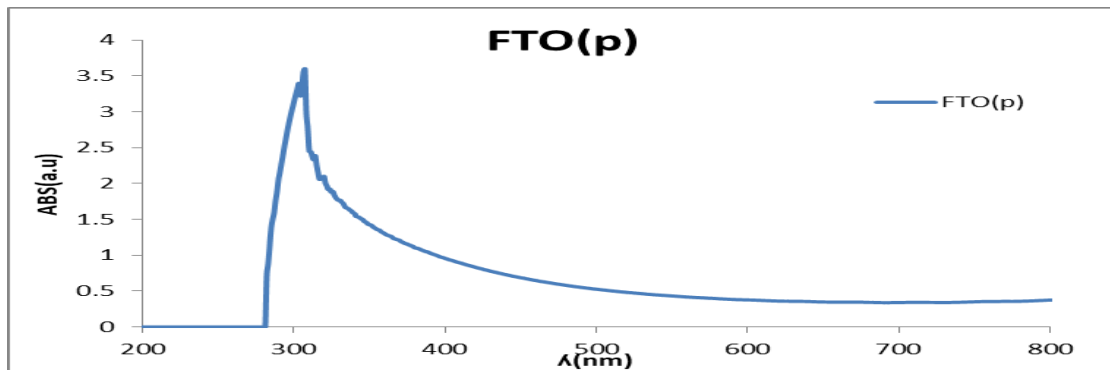


Figure (6): Optical absorption spectrum of the FTO substrate.

#### 3-3-2-2 Optical absorption spectrum of ZnS(p):

The optical absorption spectrum of the semiconductor ZnS(p) was measured using a UV-Vis spectrometer, as shown in Figure (7). It shows the presence of several optical absorption peaks corresponding to the wavelengths (371-422-460- 527-658 nm), indicating the presence of multiple impurity levels within the energy gap formed because of doping. The main absorption peak is concentrated at the wavelength (422) nm corresponding to the energy (2.93) ev, meaning that doping of the semiconductor ZnS led to a decrease in the energy gap



from (3.65) eV by (0.72) eV with the presence of additional impurity levels within the forbidden range width.

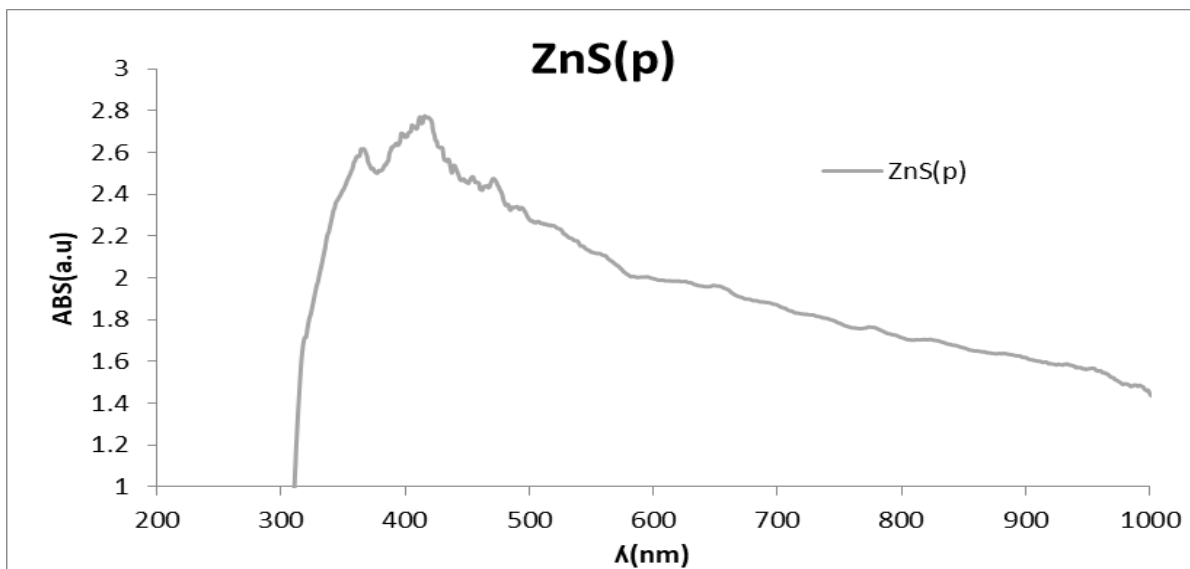


**Figure (7): Optical absorption spectrum of the semiconductor ZnS(p).**

### 3-3-2-3 Optical absorption spectrum FTO(P)/ZnS(p):

The optical absorption spectrum of the FTO(P)/ZnS(p) heterojunction was measured as shown in Figure (7). The optical absorption spectrum of the junction shows the presence of several optical absorption peaks within the visible and infrared ranges corresponding to wavelengths (356-369-409-431-458-512-570nm). By comparing these peaks with the optical absorption peaks of the formed zinc sulfide, it is noted that new optical absorption peaks are formed because of the overlap of energy levels during the deposition process in addition to the repositioning of the impurity levels within the forbidden range width of the semiconductor ZnS(p).

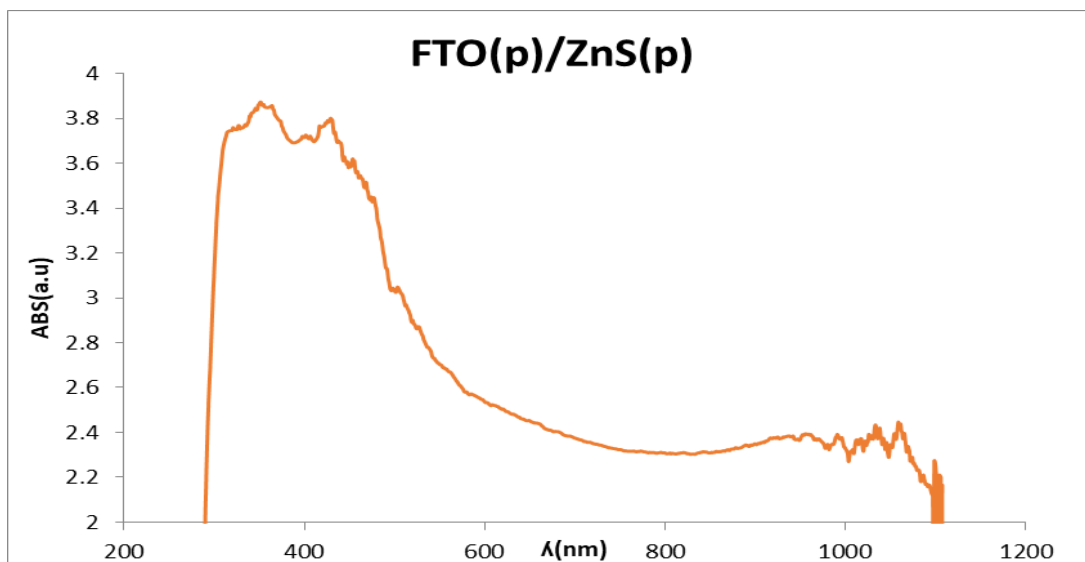


Figure (8): Optical absorption spectrum of the FTO(P)/ZnS(p) junction.

### 3-3-2-4 Optical fluorescence spectrum: FTO(p)/ZnS(p)

Figure (9) shows the optical fluorescence spectrum of the FTO(p)/ZnS(p) heterojunction using a (sinco) optical fluorescence spectrometer using an excitation wavelength of (220) nm. Figure (9) also shows the presence of two adjacent broad fluorescence peaks corresponding to wavelengths (375-400) nm, with the presence of side fluorescence peaks (416) nm and (364) nm.

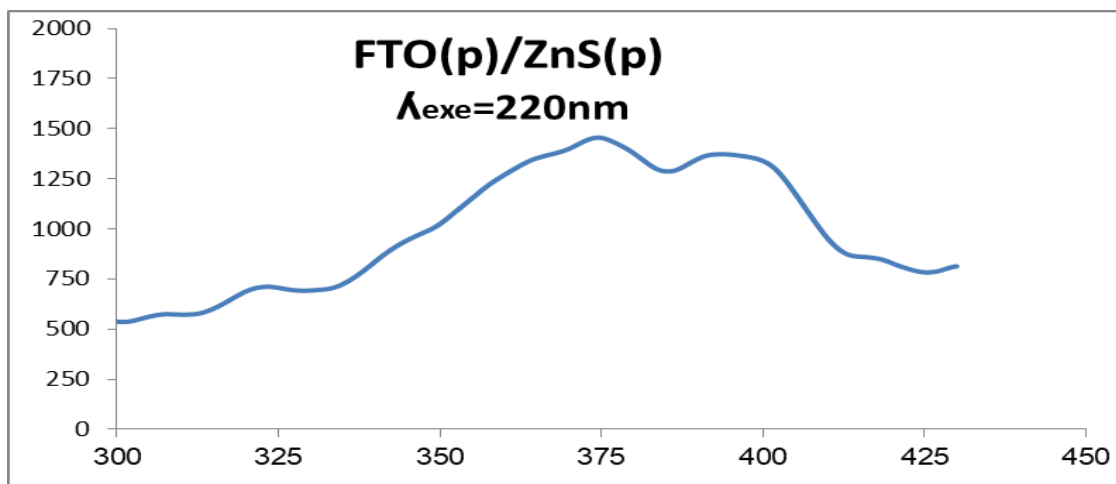


Figure (9): Photofluorescence spectrum of the FTO(p)/ZnS(p) heterojunction.



### 3-3-3 Electrical properties:

#### 3-3-3-1 Determining the type of semiconductor for the FTO(p)/ZnS(P) sample:

Confirming the type of the ZnS self-semiconductor deposited on the FTO(p) chip using the gain and phase analyzer by studying the changes in the reciprocal square of the electrical capacitance of the prepared ZnS semiconductor as a function of the applied potential, at a fixed frequency (32.44) Hz at room temperature.

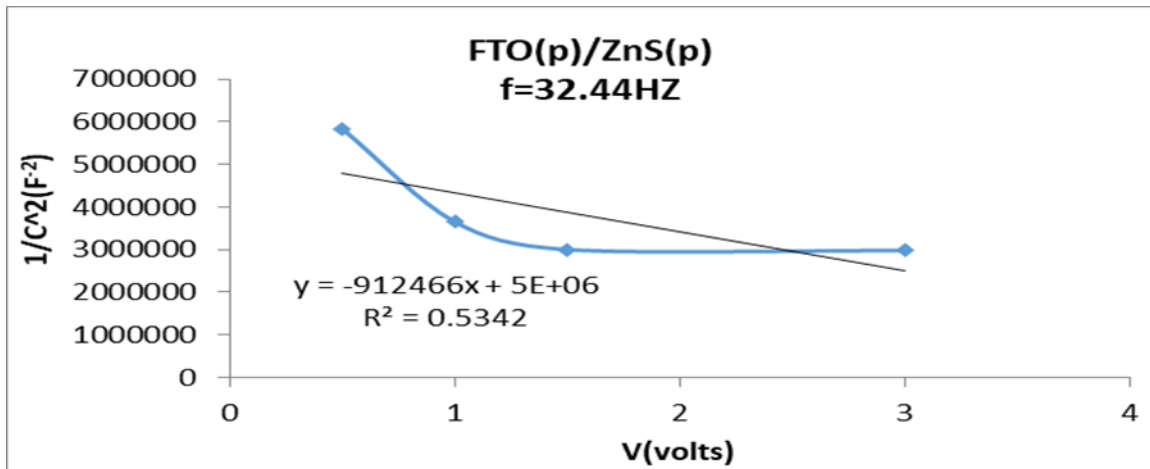


Figure (10): Changes in  $1/C^2$  as a function of voltage at a fixed frequency for the FTO(p)/ZnS(P) sample.

By plotting the changes in the reciprocal of the square of the electrical capacitance with the potential based on the following relationship, the type of semiconductor was determined as shown in Figure (10) [13]:

$$\frac{1}{C^2} = \frac{2}{e \cdot Q \cdot d} \cdot \frac{1}{N \cdot N_a} \cdot V$$



Where  $N_d$  is the density of donor atoms,  $N_a$  is the density of acceptor atoms,  $\Psi$  is the height of the potential barrier between the formed grains, and  $V$  is the potential applied to the ZnS sample. It is noted from the figure that the slope of the line is negative, which indicates that  $N_a \gg N_d$ , i.e. the density of acceptor atoms is much greater than the density of donor atoms, and therefore the prepared ZnS semiconductor has a P-type conductivity.

### 3-3-3-2 Study of the (I-V) characteristic of the FTO(p)/ZnS(p)/Si(n) junction:

The (I-V) characteristic of the FTO(p)/ZnS(p)/Si(n) heterojunction was studied at room temperature, in forward and reverse bias conditions at different illumination intensities. A forward bias voltage ranging from (0-24) volts was applied through which the threshold voltage and saturation current were determined, and the ideality factor and its relationship to the tunneling transitions that can occur within the structure of this junction were calculated.

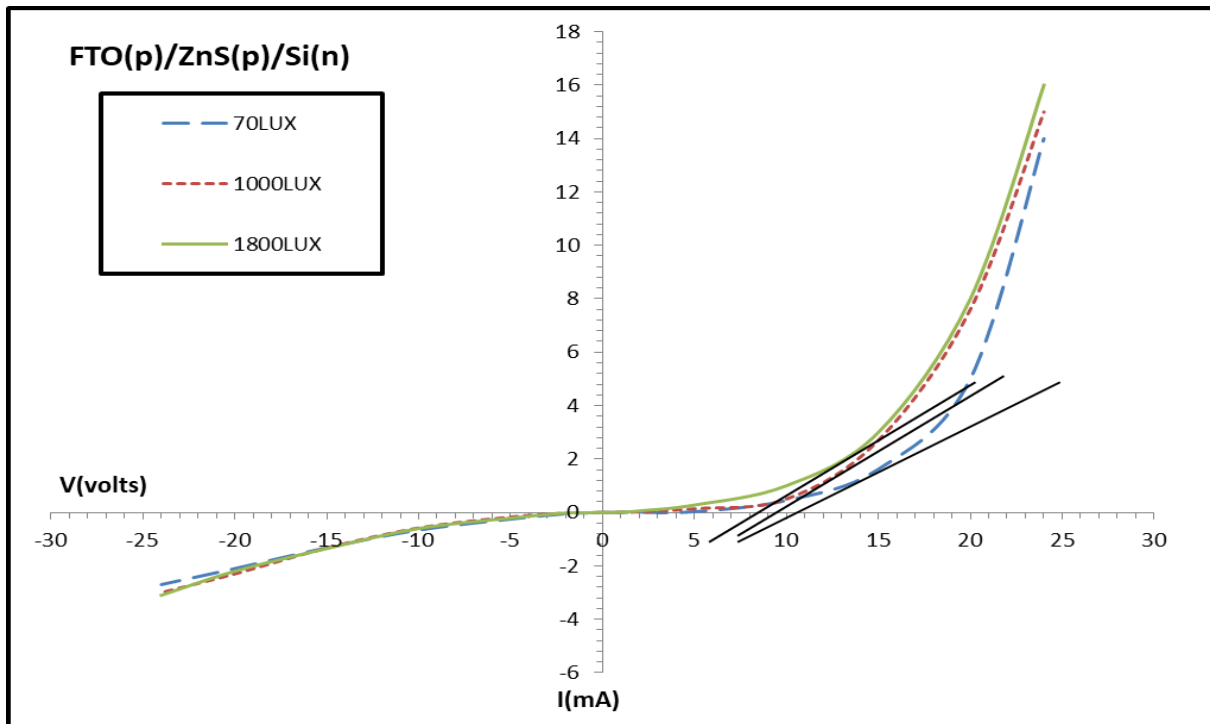


Figure (11) The (I-V) feature of the FTO(p)/ZnS(p)/Si(n) heterojunction at room temperature, in the case of forward and reverse bias at different illumination intensities.



Figure (11) shows the effect of photoexcitation on this junction, where the threshold potential value decreased when the junction surface was illuminated, with the saturation current remaining constant in the case of reverse bias, which is identical to the case of the diode junction [14]. While drawing the tangent to the graphs for each illumination intensity for the (I-V) feature, the threshold potential was determined at each illumination intensity on the prepared junction as in Table (1).

**Table (1) Threshold potentials and saturation current for each illumination intensity on the FTO(p)/ZnS(p)/Si(n) junction**

illumination intensity (LUX)	V <sub>0</sub> (volts)	I <sub>0</sub> (mA)
700	11	2.7
1111	9	3
1011	7	3.1

The ideality factor of this junction was calculated to know the mechanism controlling electrical tunneling within this structure by taking the values of the current and potential in the case of reverse bias at an illumination intensity of 1800LUX and using the Schottky relation [15]:

$$I = I_0 \left( \exp\left(\frac{eV}{nKT}\right) - 1 \right)$$

Since  $e^{(eV/nkT)} \gg 1$  neglect (1) within the parentheses in the previous relation and by taking the logarithm of both sides of the relation:

$$\ln(I) = \frac{eV}{nRT} + \ln(I_0)$$

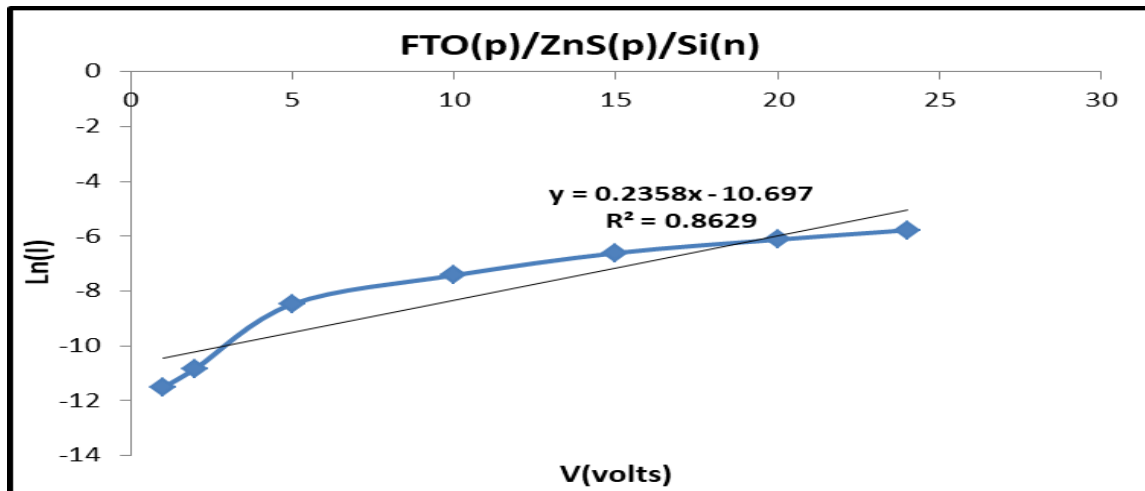
Where:

$$\frac{eV}{nRT}$$



$n$  is the ideality factor,  $I_0$  is the reverse saturation current,  $e=1.6 \times 10^{-19} \text{C}$  is the electron charge,  $K=1.3806 \times 10^{-23} \text{J/K}$  is the Boltzmann constant,  $T=300 \text{K}$  is the absolute temperature. Draw the logarithm of the current changes with the applied potential as shown in Figure (12).

**Figure (12):** shows the changes in the logarithm of the current with the potential in the



case of reverse bias at a light intensity of 1800LUX

where the slope represents:

Therefore, the value of the ideality factor is  $n=163$

- If the ideality factor is equal to (1), the dominant current is the injection current of minority charge carriers into the neutral regions of the junction, and if the ideality factor is equal to (2), the dominant current is the recombination mechanism of carriers in the space charge region, but if the ideality factor is greater than (2), the dominant current is the tunneling current [16].
- The value of the ideality factor in this heterogeneous junction is very high, which indicates the dominance of electronic transitions with tunneling effect.



#### 4- Conclusions:

- ❖ A heterojunction of FTO(p)/ZnS(p)/Si(n) was prepared in a simple and easy way.
- ❖ Atomic force microscopy (AFM) showed surface images of the FTO(p)/ZnS(p) sample with dimensions of (48.5 $\mu$ m $\times$ 48.5 $\mu$ m), where the average atomic clusters appeared (89.3) nm with the appearance of a semi-homogeneous granular structure, and the average surface heights of the granular cluster on the surface of the junction was (90.7) nm, indicating the formation of a homogeneous structure.
- ❖ X-ray diffraction measurements showed the crystallization of the FTO(p)/ZnS(p) compound according to the hexagonal structure by electrochemical deposition method.
- ❖ The optical absorption spectrum of the FTO(P)/ZnS(p) sample showed several optical absorption peaks in the visible and infrared range corresponding to several wavelengths, because of the overlap of energy levels during the deposition process in addition to the repositioning of the impurity levels within the forbidden band width of the ZnS(p) semiconductor.
- ❖ The type of the FTO(p)/ZnS(p) semiconductor was confirmed practically by studying the changes in the reciprocal square of the electrical capacitance as a function of the applied potential.
- ❖ The (I-V) feature of the FTO(p)/ZnS(p)/Si(n) heterojunction showed a decrease in the threshold potential value when illuminating the junction surface, with the saturation current remaining constant in the reverse bias case, which is identical to the diode junction case.
- ❖ The ideality factor of this junction was calculated to know the mechanism controlling the electrical tunneling transport within this structure, it was very high, indicating the dominance of electronic transitions with tunneling effect.

#### References:

- [1] Alferov, Z.I. The history and future of semiconductor heterostructures. *Semiconductors* 32,1– 14(1998). <https://doi.org/10.1134/1.1187350>
- [2] V K Mukhomorov 'Bipolaron formation and interpolaron interactions in dielectric layers' 2009 *Phys. Scr.* 79 065704, DOI 10.1088/0031-8949/79/06/065704
- [3] Chopra, K.L., Das, S.R. (1983). Photovoltaic Behavior of Junctions. In: Thin Film Solar Cells. Springer, Boston, MA. [https://doi.org/10.1007/978-1-4899-0418-8\\_33](https://doi.org/10.1007/978-1-4899-0418-8_33). A. I. GUBANOV, *Zh. Tekh. Fiz.* 22, 729 (1952).
- [4] Herbert Kroemer' Nobel Lecture: Quasielectric fields and band offsets: teaching electrons new tricks 'Rev. Mod. Phys. 73, 783 – Published 22 October 2001



- [5] R. L. Anderson' Electronic Structure of Semiconductor Heterojunctions, 1988, Volume 1 ISBN : 978-90-277-2824-1
- [6] R.L. Anderson' Experiments on Ge-GaAs heterojunctions', *Solid State Electron.* 5, 341 (1962).
- [7] W. Shockley, "The theory of p-n junctions in semiconductors and p-n junction transistors," in *The Bell System Technical Journal*, vol. 28, no. 3, pp. 435-489, July 1949, doi: 10.1002/j.1538-7305.1949.tb03645.x.
- [8]. F. H. Jneed, M. A. Batel, 2011, Tin oxide n- type semiconductor inverted to p- type semiconductor prepared by Sol-gel method, ELSEVIER, P:3.
- [9]. O.K. ECHENDU ,D.G. DISO,F. FAUZI," Characterization of n-Type and p-Type ZnS Thin Layers Grown by an Electrochemical Method' *Journal of Electronic Materials*, Vol. 42, No. 4, 2013.
- [10]. Sovann Khan, Joon Soo Han, Seung Yong Lee, and So-Hye Cho ' ZnS Nano-Spheres Formed by the Aggregation of Small Crystallites and Their Photocatalytic Degradation of Eosin B.' *Chinese Journal of Chemistry* · February 2017 DOI: 10.1002/cjoc.201600725.
- [11].Abdel-Rahim, M., Haiz, M. & Alwany, A. E. B. he efect of composition on structural and optical properties of ZnSe alloys. *Opt. Laser Technol.* 47, 88–94 (2013).
- [12]. Abdel-Rahim, M., Haiz, M. & Alwany, A. E. B. Inlucence of annealing on the structure and optical properties of Zn<sub>40</sub>Se<sub>60</sub> thin Films. *Opt. Laser Technol.* 44, 1116–1121 (2012).
- [13]. Bueno, P. R., Cassia-Santos, Garcia-Belmonte, G., Nature of the Schottky-type barrier of highly dense SnO<sub>2</sub> systems displaying nonohmic behavior, *Journalof Applied Physics* 88, 65456548(2000).
- [14]. A.Minnich, M. Dresselhaus,Z. Ren,G. Chen,"**Bulk nanostructured thermoelectric materials: current research and future prospects**". *Energ Environ Sci* **2009**, 2 (5), 466-479. [15].M.A.Batal, Lubna Alnaami "**Fabricate a heterojunction ZnS/ with ideal factor larger than "2"**" R.J.of Aleppo Univ. Basic Science Series , No.810. 2015.
- [16]. S.M. Sze, "**Physics of Semiconductor Devices**", John Wiley and Sons,Berlin, 1981.